THE ARCHIVE OF MECHANICAL ENGINEERING

Vol. L 2003 Number 2

**Key words:** *crane, optimisation, interpolation, sensitivity, positioning*

*ANDRZEJ MACZYŃSKI**)

# DETERMINATION OF DRIVE FUNCTIONS OF SLEWING OF A MOBILE CRANE WHICH MINIMIZE LOAD OSCILLATIONS

A method of determination of drive functions of slewing of a mobile crane's upper structure is presented in the paper. The purpose of their determination is to reduce load oscillations at the end of the motion. Drive functions for selected angles and durations of slewing have been calculated using a simple model of the crane and dynamic optimisation. Drive functions for intermediate angles have been determined by means of interpolation. Results of numerical simulations executed for the model of the crane are presented, taking into consideration flexibilities and damping in the cranes subsystems. Results obtained for drive functions determined using optimisation and interpolation algorithms are compared. An attempt to determine sensitivity of load positioning to selected operating parameters is also presented. Introduction of the notion of a positioning quality coefficient is proposed.

## 1. Introduction

During the slewing motion of a crane, the transferred load deflects from the vertical. This deflection causes load swings. Their character is similar to swing of a spherical pendulum. After the end of the motion, the load swings freely. Because there is relatively slight damping in the system, these oscillations can remain for a fairly long time. For efficiency and safety of work carried out with cranes, it is desirable to eliminate or at least substantially reduce these final oscillations. Improvement of safety is especially vital, because a considerable number of fatal accidents at building sites are connected with crane usage [1]. Therefore, the problem of reduction of load oscillations is the main topic of many papers. The proposed methods

*) *Uniwersity of Bielsko-Biała Faculty of Mechanical Engineering and Computer Sciences, Willowa 2, 43-309 Bielsko-Biała, Poland; E-mail: amaczynski@ath.bielsko.pl*

of influence on the load in order to reduce its oscillations can be divided into three basic groups:

1. additional mechanical systems,
2. application of one of the other crane drives (besides the slewing motion) i.e. the servo-motor changing crane radius or the drive of the hosting winch,
3. application only the slewing motion with the time course of the drive function appropriately calculated beforehand.

One of the solutions from the first group is presented in [2]. Balachandran et al. propose and describe a concept which they call a mechanical filter. This is based on the premise that, by controlling the pivot point about which the load oscillates, one can effectively suppress crane-load oscillations.

The paper of Abdel-Rahman and Nayfeh [3] can be included in the second group. Results demonstrating that rope-length can be changed to reduce load oscillations are presented there. Significant reductions can be obtained via an appropriate choice of the reeling/unreeling speed. Also Sakawa et al. [4] propose the optimal control of a rotary installed crane which performs two kinds of motion (slewing and hoisting) at the same time. The optimal control which transfers a load to a desired place as fast as possible and minimizes the oscillations of the load during the transfer as well as at the end of the motion is calculated.

Paper [5] belongs to the third group. Kłosiński applies experience gained during work connected with methods of load positioning in a gantry crane. Parker et al. [6] compare different methods of determination of the drive function of the slewing motion of a jib crane. A dynamic programming method has been employed to obtain the hub angular acceleration history for a variable load-line jib crane producing residual oscillation free payload motion. It has been shown that the hub angular acceleration could also be postulated using a bang-coast-bang shape to achieve the desired residual oscillation free behaviour. The parameters of this shape have been calculated using a recursive quadratic programming numerical optimisation code.

The application of additional mechanical systems to minimize load oscillations is associated with higher cost and more complicated structure of the crane, and simultaneous, synchronous use of two or more drives causes considerable problems with their control. However, methods from the third group are relatively cheap and easy to use. The method presented in the paper belongs to this category. It is based on the assumption that the drive function can be calculated by means of optimisation. Because numerical efficiency has to be ensured, this optimisation problem has been solved for a simple model of a crane. Nevertheless, the function is also intended to guarantee reduction of load oscillations at the end of the motion for a more complex model and for a real crane. It is an inconvenience that the method requires each time previous calculation of the course of the drive function for specific operating parameters, especially for the specific angle of slewing. In order to avoid this, the desired functions are calculated only for selected angles, whereas functions for remaining angles may be determined by means of interpolation. The drive functions calculated for specific angles would be permanently stored in the crane control system memory (forming the so-called „map of basic slewing functions"). Functions for intermediate angles would be determined by the control system in real time.

The angle and the time of the slewing are not the sole operating parameters which should be defined in the optimisation process of the slewing function. Mass of the load and length of the rope between the end of the jib and the load are particularly important. During the construction of the „map of basic slewing functions", the knowledge of sensitivity of load positioning to these remaining parameters is essential. Therefore an attempt to determine sensitivity of load positioning to changes of nominal mass (assumed in optimisation) and length of the rope has been undertaken in this paper. In order to enable quantitative analysis of positioning quality, the introduction of a special coefficient has been proposed.

## 2. Optimisation of drive functions

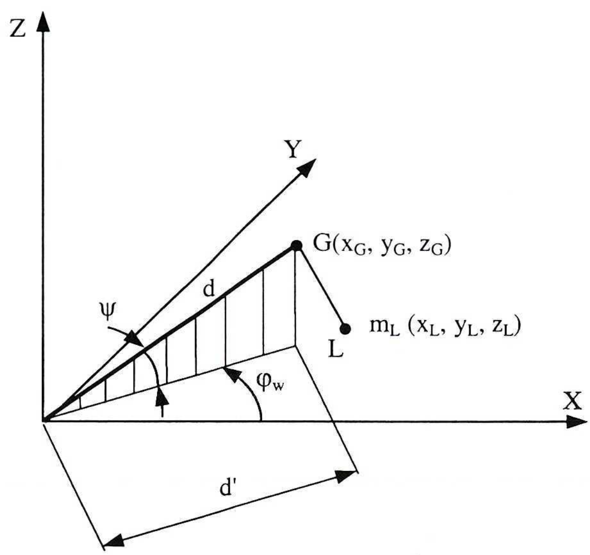


Fig. 1. Model of crane applied in optimisation problem

It has been mentioned that, in order to ensure numerical efficiency, optimisation of the slewing function was carried out for the simplified model of the crane. A completely stiff supporting structure of the crane has been assumed. In the result of these assumptions, a model with three degrees of freedom has been obtained (Fig. 1). Then equations of the load can be presented in the following form:

$$m_L \ddot{x}_L = S \frac{x_G - x_L}{L_L} \tag{1}$$

$$m_L \ddot{y}_L = S \frac{y_G - y_L}{L_L} \tag{2}$$

$$m_L \ddot{z}_L = S \frac{z_G - z_L}{L_L} - m_L g \tag{3}$$

where
$m_L$ – mass of the load,
$S$ – force in the rope GL,
$L_Ł$ – length of the rope GL.

There are four unknowns $x_L$, $y_L$, $z_L$, $S$ in equations (1) – (3). They must be supplemented by a constraint equation in the form:

$$|GL|^2 = [x_G - x_L]^2 + [y_G - y_L]^2 + [z_G - z_L]^2 = const \tag{4}$$

Equation (4) means that the length of rope (spherical pendulum) is constant. Moreover, with reference to Fig.1, the following relations occur:

$$\begin{cases} x_G = d \cos\psi \cos\varphi = d' \cos\varphi \\ y_G = d \cos\psi \sin\varphi = d' \sin\varphi \\ z_G = d \sin\psi = const \end{cases} \tag{5}$$

It has been also assumed that for $t \in \langle t_0, T \rangle$ the function $\varphi_w(t)$ can be approximated by means of third-order spline functions (Fig. 2). As decisive variables in the optimisation problem we consider the components of the vector below:

$$\mathbf{X} = [\varphi_{w,1}, \varphi_{w,2}, \ldots, \varphi_{w,n_d-1}]^T \tag{6}$$

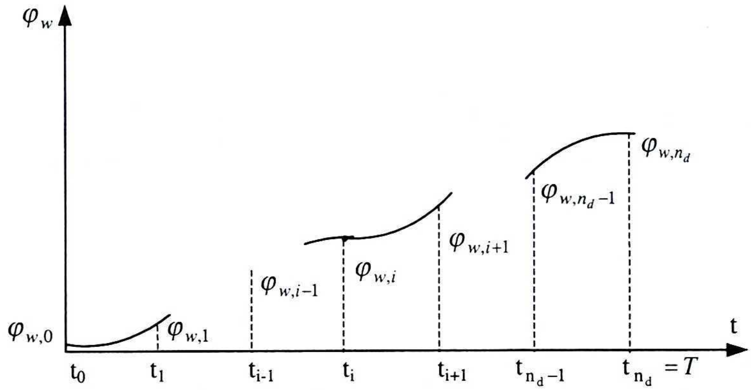


Fig. 2. Function $\varphi_w(t)$ approximated by spline functions

i.e. the variables of the slewing function at the selected points of the interval. The objective function has been defined as follows:

$$F = C_1 \cdot \frac{1}{2} m_L \cdot \mathbf{v}_{\mathbf{LT}}^2 + C_2 \cdot \|\mathbf{r}_{\mathbf{LT}} - \mathbf{r}_{\mathbf{LF}}\|^2 \tag{7}$$

where

$\mathbf{r}_{\mathbf{LT}} = \mathbf{r}_{\mathbf{L}}|_{t=T}$, $\mathbf{v}_{\mathbf{LT}} = \mathbf{v}_{\mathbf{L}}|_{t=T}$ – vectors of load coordinates and velocity for $t = T$,

$\mathbf{r}_{LF}$ – vector of expected load coordinates for $t = T$,

$C_1$, $C_2$ – coefficients (weights).

This function means that one can expect that at the end of the slewing motion the load is at a particular point in space and, furthermore, its kinetic energy is minimal. Therefore, the precise formulation of the optimisation problem can be expressed in the following terms: find the minimum of function $F$ presented by (7) by selection of values $\varphi_{w,1},\ldots,\varphi_{w,n_d-1}$ that are the components of vector $\mathbf{X}$ (6). The Nelder – Meads method has been used for its solution. Like most optimisation methods, this is also sensitive to selection of initial approximation. In the present paper, it has been assumed that initial approximation of vector $\mathbf{X}$:

$$\mathbf{X_0} = [\varphi_{w,1,0},\ldots,\varphi_{w,n_d-1,0}]^T \tag{8}$$

is obtained based upon the formulae:

$$\varphi_{w,i,0} = \varphi_w(t_i) = \begin{cases} \dfrac{8\varphi_{\mathrm{w,max}}}{T^4} t^3(-t+T) & when \quad t \le \dfrac{T}{2} \\ \dfrac{8\varphi_{\mathrm{w,max}}}{T^4} (t-T)^3 \cdot t & when \quad t > \dfrac{T}{2} \end{cases} \tag{9}$$

This function fulfils the following conditions:

$$\varphi_w(0) = 0 \qquad \dot{\varphi}_w(0) = 0$$
$$\varphi_w\left(\frac{T}{2}\right) = \frac{1}{2}\varphi_{w,\max} \tag{10}$$
$$\varphi_w(T) = \varphi_{w,\max} \; \dot{\varphi}_w(T) = 0$$

where $\varphi_{w,\max}$ is the final angle of the slewing motion.
The function chosen in this way ensures that courses of $\varphi_w = \varphi_w(t)$ and $\dot{\varphi}_w = \dot{\varphi}_w(t)$ curves are smooth.

## 3. Determination of drive functions for selected angles of slewing

Numerical simulations have been performed for technical data of a typical crane with lifting capacity up to 30 Mg. Mass of the load $m_L$ was equal to 3000 kg, crane radius $d$ about 8.6 m, length $L_L$ about 10 m.

Optimisation of the drive function has been executed for different numbers of decisive variables (6). Finally, in the presented examples, the four-element vector of decisive variables has been employed. This number of decisive variables ensures sufficient numerical efficiency and simultaneously gives good precision of load positioning. The average time of optimisation did not exceed 2 minutes on a PC computer with the Intel® Pentium® IV 1.8 GHz processor. Values of coefficients $C_1$ and $C_2$ have been determined during numerical simulations. The main criterion of this determination was the best quality of positioning of the load at the end of the slewing motion. Optimal drive functions for two cases of motion have been determined:

I. 90° slewing over a period of 15 s,
II. 60° slewing over a period of 12 s.

The following figures present: time courses of the input angle of the upper structure slewing $\varphi_w(t)$ (Figs. 3, 4); slewing speed $\dot{\varphi}_w(t)$ (Figs. 5, 6); projections of trajectories of the load $L$ on the plane of the ground (Figs. 7, 8) and time courses of kinetic energy of the load (Figs. 9, 10) for initial approximation of drive functions (9) and optimal drive functions. In cases shown in Figs. 7 and 8 the origin of the coordinate system is not in the axis of rotation of the upper structure (like in Fig. 1) but in the mass centre of the chassis (Fig. 11). This point is at the distance of 2.6 m along axis X. The time of observation of load motion was 30 s.

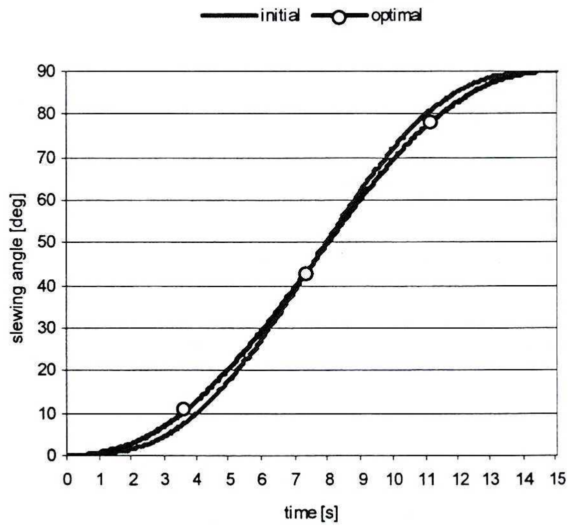


Fig. 3. Time course of input angle of slewing for case I

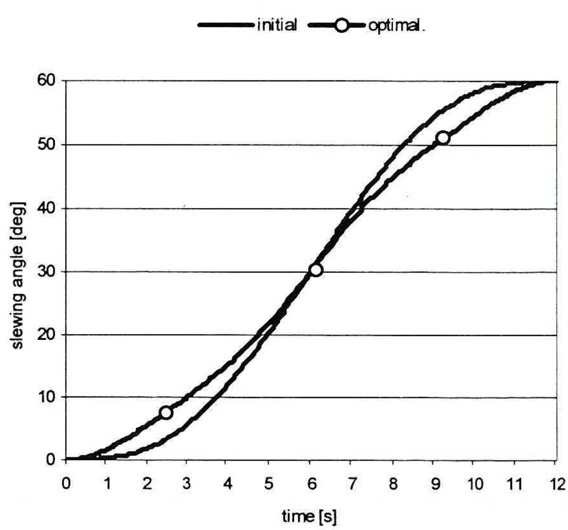


Fig. 4. Time course of input angle of slewing for case II

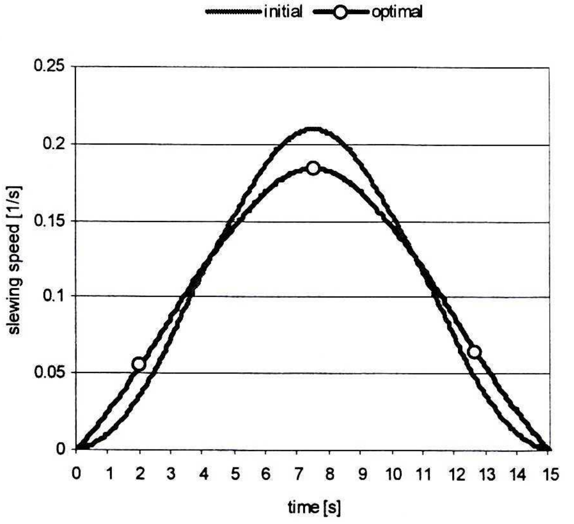


Fig. 5. Slewing speed for case I

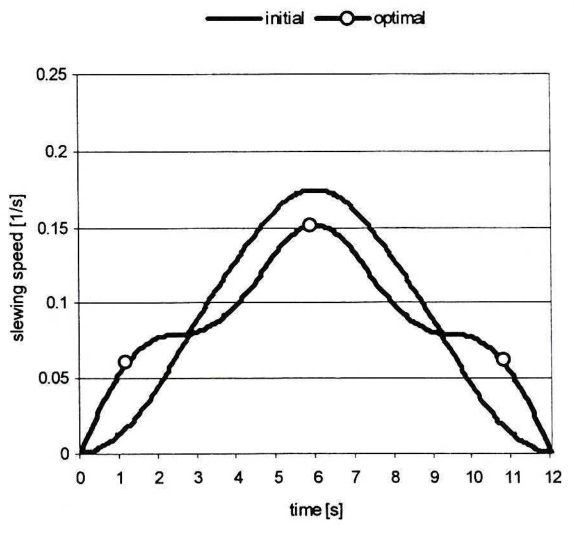


Fig. 6. Slewing speed for case II

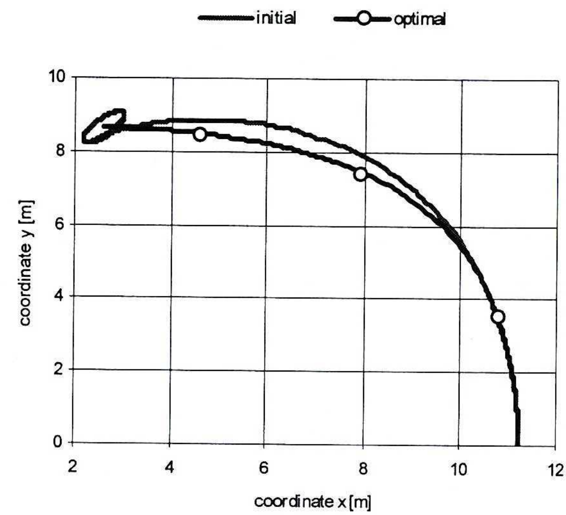


Fig. 7. Projection of load trajectories on the plane of the ground – case I

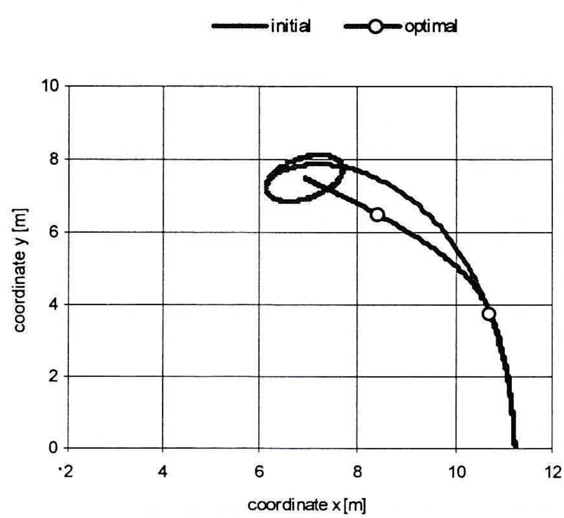


Fig. 8. Projection of load trajectories on the plane of the ground – case II

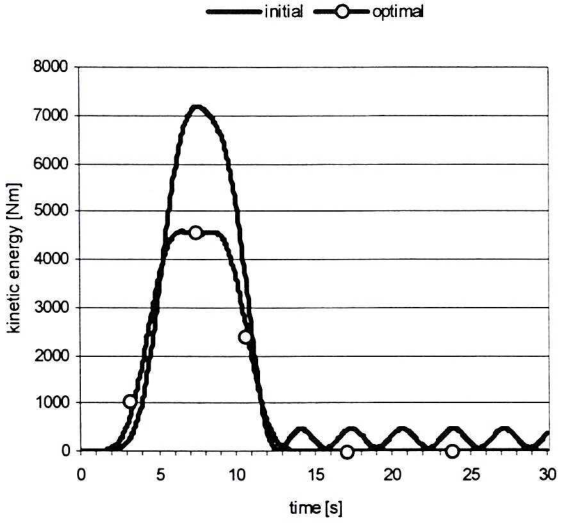


Fig. 9. Time course of kinetic energy of the load – case I

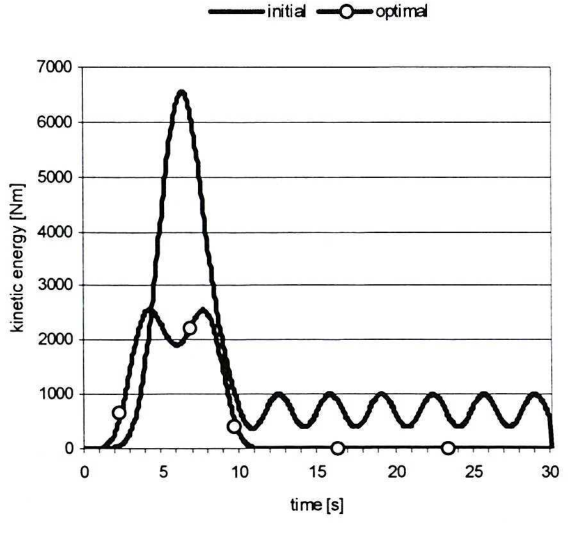


Fig. 10. Time course of kinetic energy of the load – case II

## 4. Load positioning for the model taking into account flexibilities of the system

In order to examine the efficiency of application of optimal drive functions in quasi-real conditions, numerical simulations using another model that takes into account flexibility of the crane's supported structure and damping in selected subsystems (Fig. 11) have been performed. The model is intended for dynamic analysis with the following inputs:

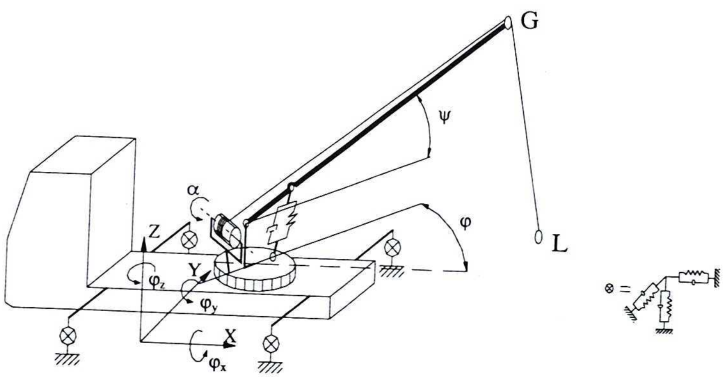


Fig. 11. Model of a mobile crane

– slewing of a crane's upper structure (angle $\varphi$),
– lifting and lowering of a load by means of a hoisting winch (angle $\alpha$),
– changing the length of a servo-motor which changes crane radius (angle $\psi$).

The model is presented in detail in [7], [8], [9]. The equations of motion of the crane have been derived from the Lagrange equations of the second order. After determining all necessary components of the Lagrange equations (energies, functions of energy dissipation for all subsystems of the crane and their differentials), the following system of equations of motion is obtained:

$$\mathbf{A} \cdot \ddot{\mathbf{u}} = \mathbf{F} \tag{11}$$

which can be rewritten in the form:

$$\underbrace{\begin{bmatrix} \mathbf{A}^{\mathrm{q}} & \mathbf{A}^{\mathrm{wqp}} & \mathbf{0} & \mathbf{0} \\ \mathbf{A}^{\mathrm{wpq}} & \mathbf{A}^{\mathrm{wpp}} & \mathbf{0} & \mathbf{0} \\ \mathbf{0} & \mathbf{0} & A^{b} & \mathbf{0} \\ \mathbf{0} & \mathbf{0} & \mathbf{0} & \mathbf{A}^{\mathrm{L}} \end{bmatrix}}_{\mathrm{A}} \cdot \underbrace{\begin{bmatrix} \ddot{\mathbf{q}} \\ \ddot{\mathbf{p}} \\ \ddot{\alpha} \\ \ddot{\mathbf{q}}_{\mathrm{L}} \end{bmatrix}}_{\ddot{\mathrm{u}}} = \underbrace{\begin{bmatrix} \mathbf{F}^{\mathrm{q}} \\ \mathbf{F}^{\mathrm{p}} \\ F^{B} \\ \mathbf{F}^{\mathrm{L}} \end{bmatrix}}_{\mathrm{F}} \tag{12}$$

where

$\mathbf{q} = [x_{01}, y_{01}, z_{01}, \varphi_{x1}, \varphi_{y1}, \varphi_{z1}, \varphi, \psi]^T$,

$[x_{01}, y_{01}, z_{01}, \varphi_{x1}, \varphi_{y1}, \varphi_{z1}]^T$ – vector of coordinates of the chassis,

$\mathbf{p} = [p_1, \ldots, p_m]^T$ – vector of coordinates of the jib,

$m$ – number of modes taken into consideration in modal analysis, in the plane of lifting and in the plane perpendicular to it respectively,

$\mathbf{q}_{\mathrm{L}}$ – coordinates of the load.

Equations (12) form a system of ordinary non-linear differential second-order equations for variable t with a changeable number of degrees of freedom, because phases of load lifting from the ground are taken into account. Before the equations are solved, static deflections should be determined, since these constitute initial conditions for motion of the system. The fourth order Runge-Kutta method has been used to solve the system of differential equations (12).

The results presented below have been obtained for inputs in the following forms of drive functions: the initial approximation (in accordance with (9)) and the optimal function. Both cases of the motion mentioned above, i.e. slewing by 90° (case I) and by 60° (case II) have been considered. In Figs. 12 and 13 projections of final parts of load trajectories on the plane of the ground are presented. Figs. 14 and 15 show time courses of kinetic energy of the load for slewing I and II respectively. By analysing the graphs, one can deduce that after optimisation, for the model taking into account flexibility of the supported structure, the load is not motionless at the end of the slewing, but it oscillates. However, the amplitude of these oscillations is small and in both cases it does not exceed several centimetres.

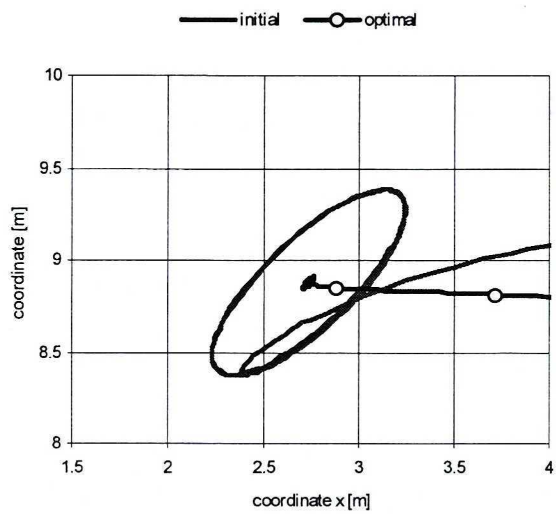


Fig. 12. Projection of final parts of load trajectories on the plane of the ground – case I

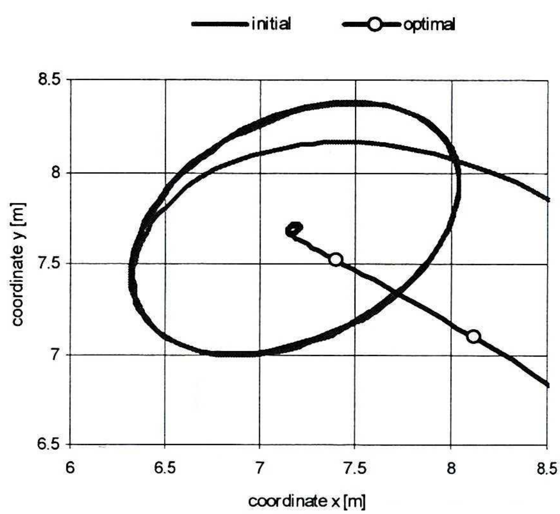


Fig. 13. Projection of final parts of load trajectories on the plane of the ground – case II

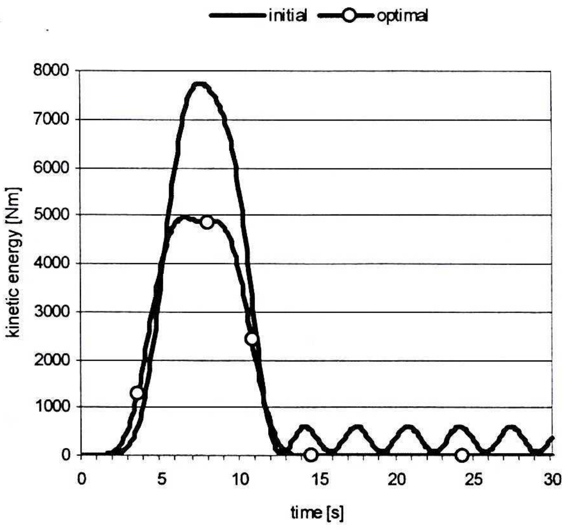


Fig. 14. Course of kinetic energy of the load – case I

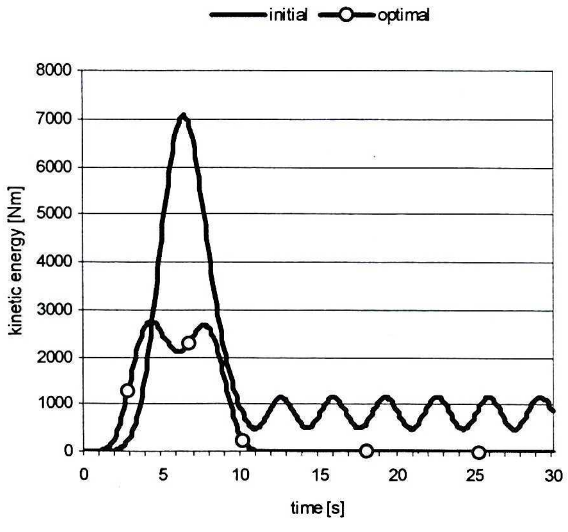


Fig. 15. Course of kinetic energy of the load – case II

## 5. Interpolation of the drive function for intermediate angles of slewing

In this section, the method and results of interpolation of the drive function for 90° slewing are presented. A linear interpolation algorithm has been used. The optimal functions for slewing by 90° and 60° (section 3) have been taken as initial (basic) functions. Because slewing by 90° was realized over a period of 15 s and slewing by 60° over a period of 12 s, it was assumed that the time of slewing by 75° is equal to 13.5 s. Next, transitional angles of slewing corresponding to elements of the vector of decisive variables (6) were determined. For slewing by 75°, they were calculated as the arithmetic mean of decisive variables of basic functions (90° and 60°). The results obtained for the interpolated function were compared with those obtained for the optimal drive function determined according to the method presented in section 2. The simulations were carried out for the model, taking into account flexibility of the supported structure presented in section 4. The following figures show: comparison of drive functions of slewing for 75° obtained using interpolation and optimisation algorithms (Fig. 16); difference between these functions (Fig. 17); projections of the complete load trajectories on the plane of the ground and of their final part, respectively, for input in the form of initial approximation (9), optimal function and interpolated function (Figs. 18 and 19); comparison of time courses of kinetic energy of the load (Fig. 20).

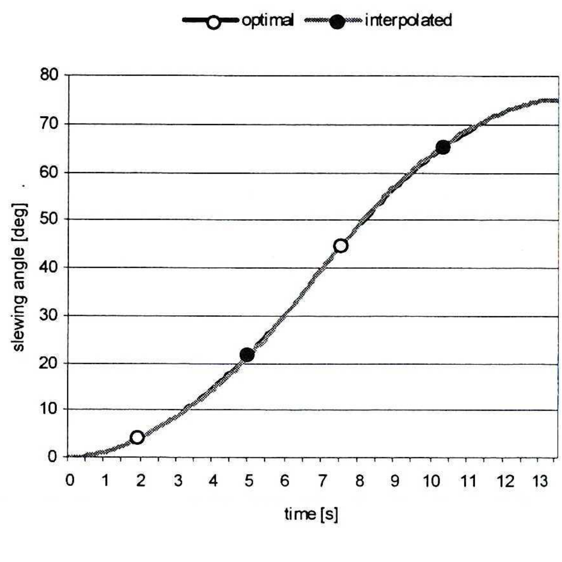


Fig. 16. Comparison of time courses of drive functions for 75° slewing

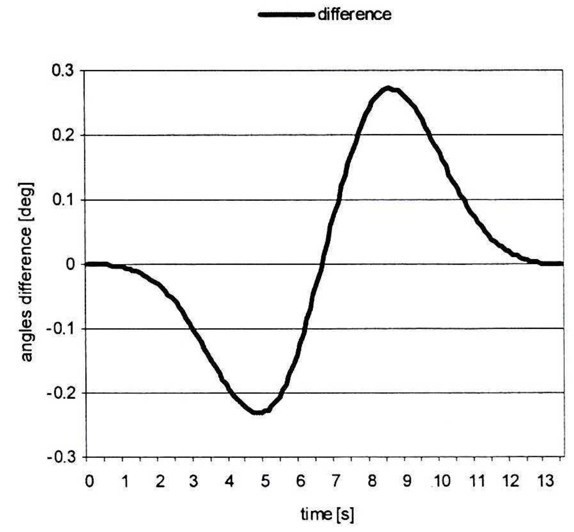


Fig. 17. Difference between optimal and interpolated functions for 75° slewing

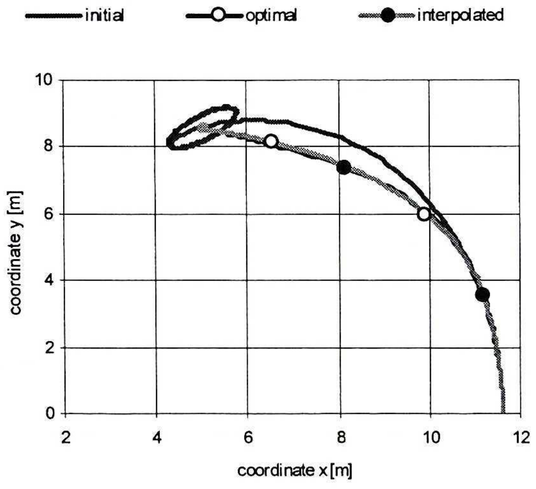


Fig. 18. Projection of load trajectories on the plane of the ground for 75° slewing

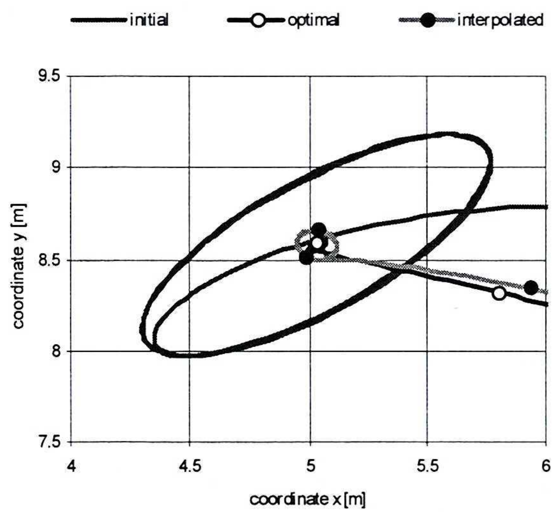


Fig. 19. Projection of final parts of load trajectories on the ground – slewing by 75°

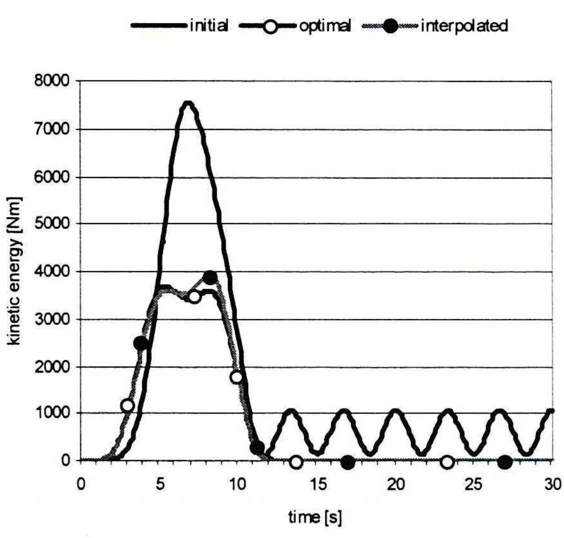


Fig. 20. Time course of kinetic energy of the load – slewing by 75°

## 6. Sensitivity of load positioning

When determining the optimal drive function of slewing, in addition to the angle of slewing, the time of the motion and the starting angle of the jib, one also has to define: mass of the load and height of load suspended, i.e. length of the rope between the end of the jib and the load. The results of calculations showing sensitivity of load positioning at the end of the motion to changes of mass of the load and length of the rope are presented bellow. The increases (5, 10, 20%) and the decreases (10, 25, 50, 75 %) of the mass of load and the increases (10, 25, 50 cm) and the decreases (10, 25, 50, 75 cm) of the length of rope in comparison to the nominal data (assumed in the optimisation task) have been analysed. Efficiency of load positioning can be easily estimated upon the basis of projections of load trajectories. However this estimation has mainly qualitative character. Thus, a quantitative coefficient describing the quality of final load positioning can be introduced. In this paper, the following definition of a quality positioning coefficient is proposed:

$$P_E = \sqrt{x_o^2 + y_o^2} \tag{13}$$

where

$x_o = |x_L - x'_{LF}|_{\max}$

$y_o = |y_L - y'_{LF}|_{\max}$

$x_L, y_L$ – coordinates x, y of the load,

$x'_{LF}, y'_{LF}$ – expected load coordinates for $t = T$,

$|x_L - x'_{LF}|_{\max}, |y_L - y'_{LF}|_{\max}$ – maximal absolute value of the difference between coordinates after the end of slewing.

Load coordinates $x'_{LF}, y'_{LF}$ expected at the time $t = T$ have been determined for static load of the crane for the specific final angle of slewing and the mass of the load. The coefficient $P_E$, for motions analysed in section 2 (simplified model, optimal drive functions), is equal to 0.14 cm. When flexibilities of the system are taken into consideration, the coefficient increases to 4.37 cm for slewing by 60° and to 4.42 cm for 90°.

The knowledge about sensitivity of load positioning is vital for construction of the „map of basic slewing functions". If sensitivity of load positioning for a selected parameter is low, the slewing of the crane can be executed for a certain range of this parameter by means of only one drive function and the positioning quality can be satisfactory. Results presented below have been obtained for the model taking into account flexibility of the supported structure.

## 6.1. Sensitivity of load positioning for basic angles of slewing

The sensitivity of load positioning for basic slewing functions, i.e. slewing by 90° (case I) and by 60° (case II) was investigated in the first place. The following figures present a comparison of projections of final parts of load trajectories on the plane of the ground for nominal parameters and an appropriately changing mass of the load and length of the rope. Figures 21, 23, 25, 27 are related to slewing for case I and Figures 22, 24, 26, 28 with case II. Figs. 21 and 23 were obtained for increased and Figs. 22 and 24 for decreased mass of the load. Similarly Figs. 25 and 26 were obtained for increased and Figs. 27 and 28 for decreased length of the rope. Moreover, the comparison of $P_E$ coefficient values for the cases analysed is presented in Table 1.

Table 1.

Comparison of $P_E$ coefficient values for basic slewing functions 90° and 60°

| Slew | Value of $P_E$ coefficient [cm] | | | | | | | | | | | | | | |
|---|---|---|---|---|---|---|---|---|---|---|---|---|---|---|---|
| | nom. | 1.05m | 1.1m | 1.2m | 0.9m | 0.75m | 0.5m | 0.25m | +10 | +25 | +50 | −10 | −25 | −50 | −75 |
| 90° | 4.42 | 4.66 | 4.90 | 5.38 | 3.94 | 3.25 | 2.18 | 1.05 | 5.97 | 8.35 | 12.5 | 2.91 | 0.78 | 2.97 | 6.26 |
| 60° | 4.37 | 4.59 | 4.81 | 5.27 | 3.91 | 3.17 | 2.19 | 1.07 | 5.74 | 7.77 | 11.1 | 3.00 | 0.95 | 2.78 | 6.45 |

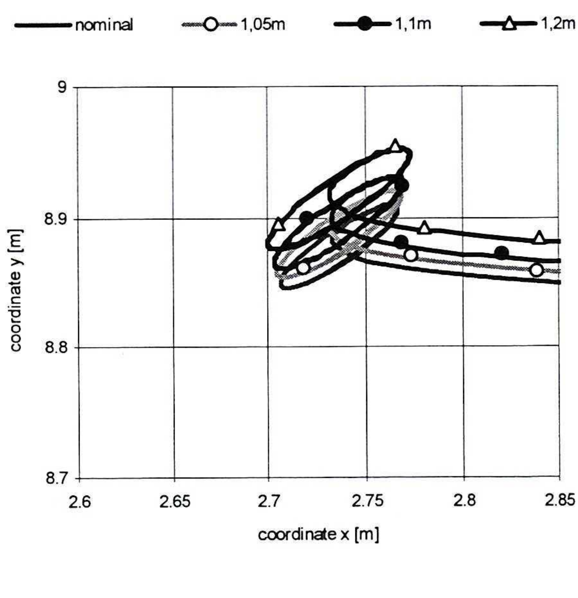


Fig. 21. Trajectories of load for increased mass – I case of motion

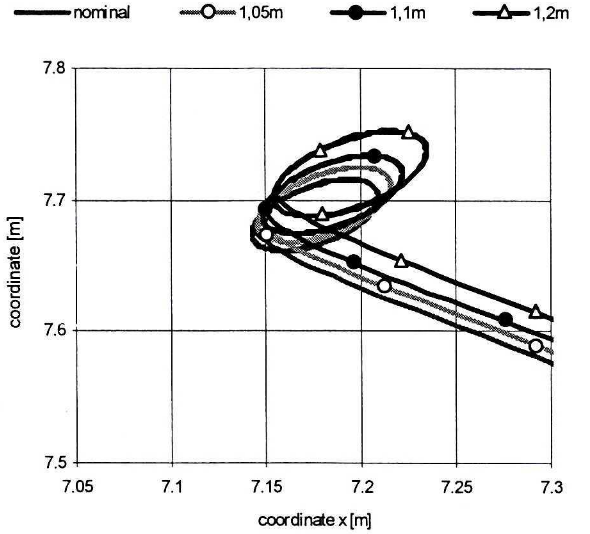


Fig. 22. Trajectories of load for increased mass – II case of motion

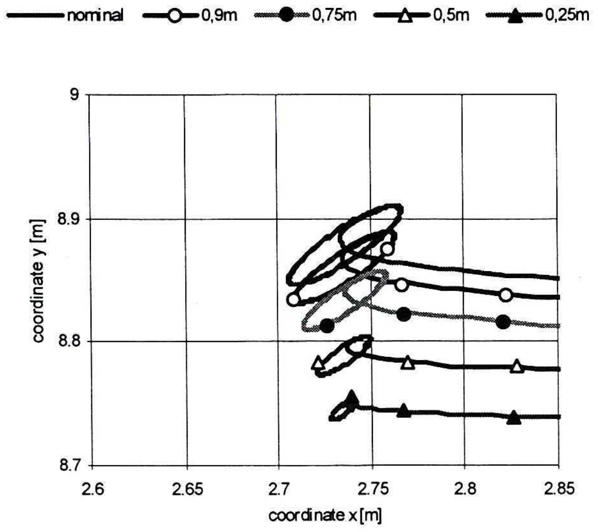


Fig. 23. Trajectories of load for decreased mass – I case of motion

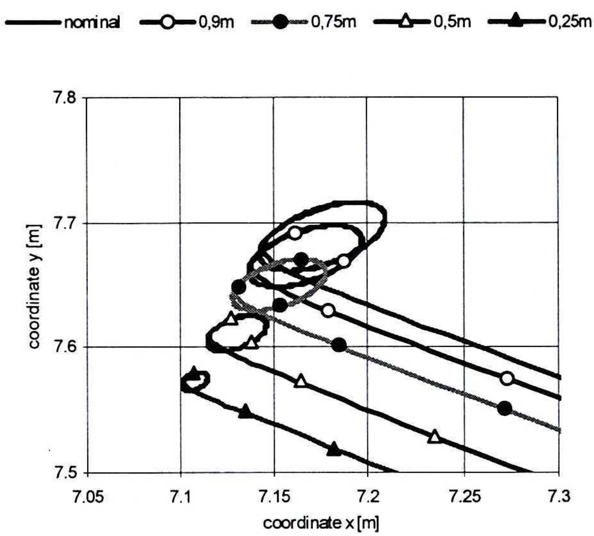


Fig. 24. Trajectories of load for decreased mass – II case of motion

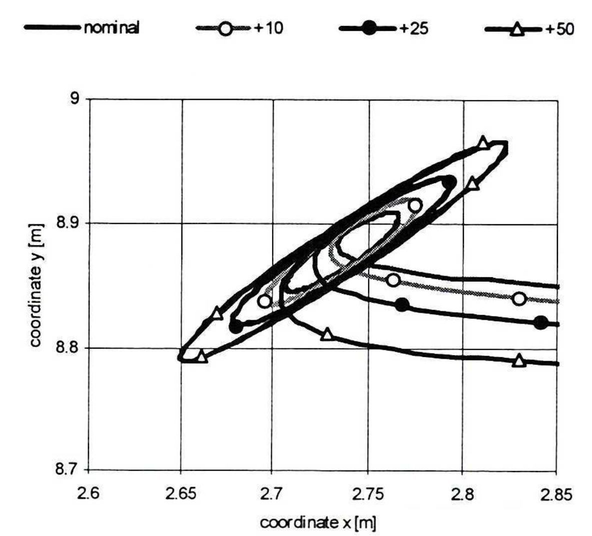


Fig. 25. Trajectories of load for increased length of the rope – I case of motion

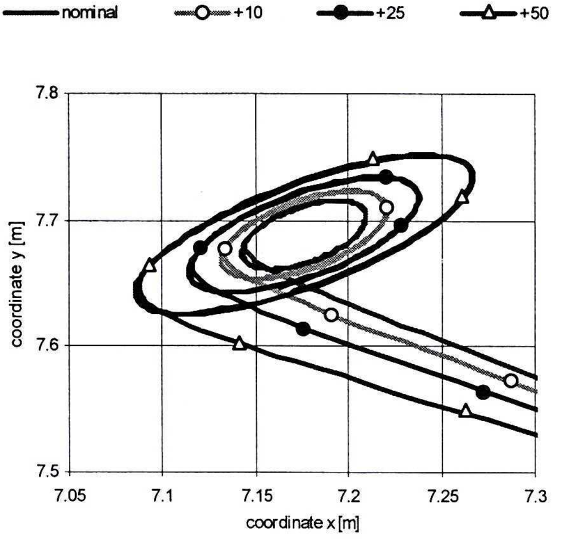


Fig. 26. Trajectories of load for increased length of the rope – II case of motion

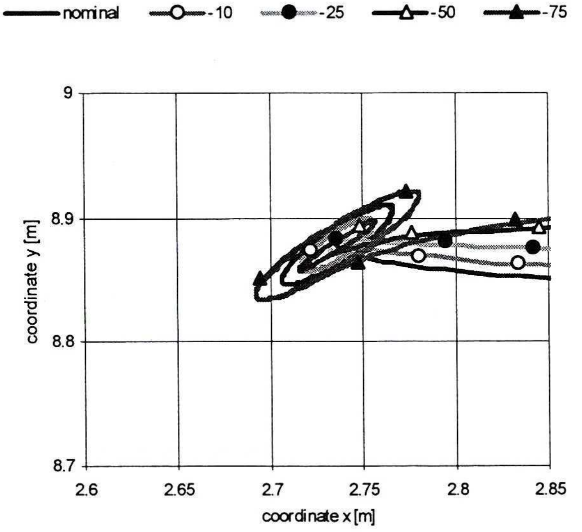


Fig. 27. Trajectories of load for decreased length of the rope – I case of motion

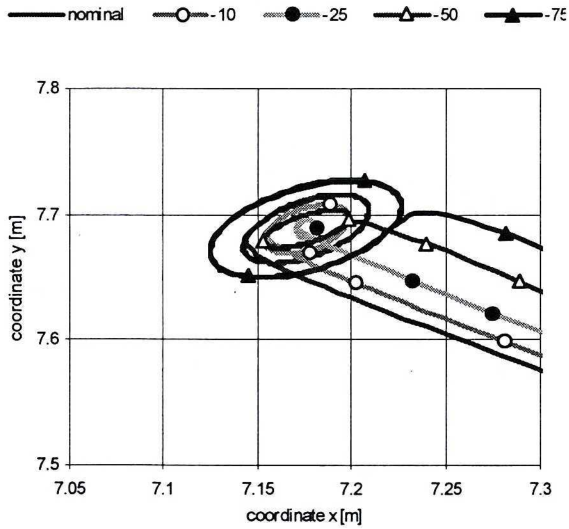


Fig. 28. Trajectories of load for decreased length of the rope – II case of motion

## 6.2. Sensitivity of load positioning for the intermediate angle

In this section, the sensitivity of load positioning at the end of the motion to changing mass of the load and length of the rope is compared. However, slewing of the upper structure by 75° is here discussed. The input of slewing has been performed by using the optimal function and the function determined by means of the interpolation algorithm in accordance with section 5. The arrangement of figures is analogous to the arrangement in section 6.1. Figures 29, 31, 33, 35 were obtained for the optimal drive function and Figures 30, 32, 34, 36 for the interpolated one. The comparison of PE coefficient values for the cases analysed is presented in Table 2.

Table 2.

Comparison of $P_E$ coefficient values for the intermediate angle of slewing – 75°

| Function | Value of $P_E$ coefficient [cm] | | | | | | | | | | | | | |
|---|---|---|---|---|---|---|---|---|---|---|---|---|---|---|
| | nom. | 1.05m | 1.1m | 1.2m | 0.9m | 0.75m | 0.5m | 0.25m | +10 | +25 | +50 | −10 | −25 | −50 | −75 |
| optm. | 4.59 | 4.77 | 5.05 | 5.51 | 4.08 | 3.39 | 2.23 | 1.12 | 6.09 | 8.37 | 12.2 | 3.10 | 0.95 | 2.98 | 6.57 |
| inter. | 11.7 | 11.7 | 11.9 | 12.1 | 11.4 | 11.2 | 10.9 | 10.7 | 12.4 | 13.9 | 16.8 | 11.1 | 10.7 | 11.1 | 13.0 |

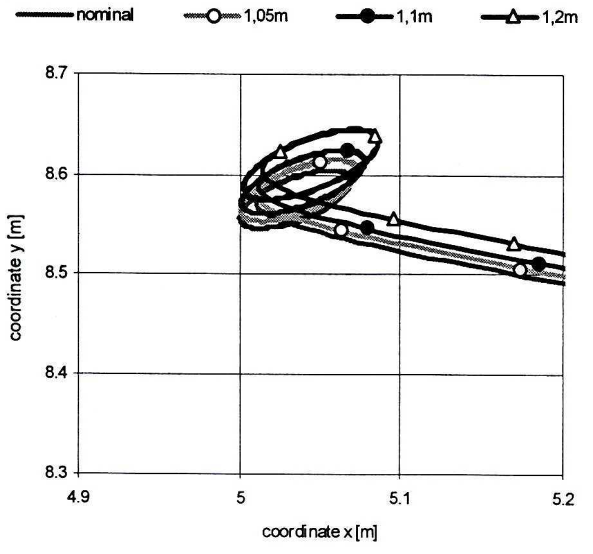


Fig. 29. Trajectories of load for increased mass – optimal drive function

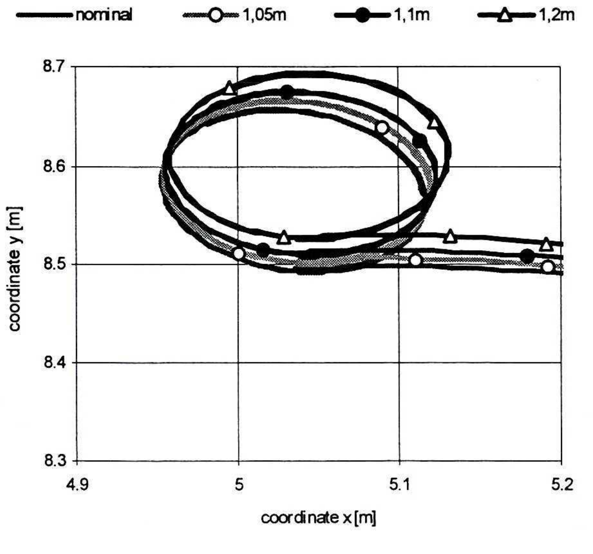


Fig. 30. Trajectories of load for increased mass – interpolated drive function

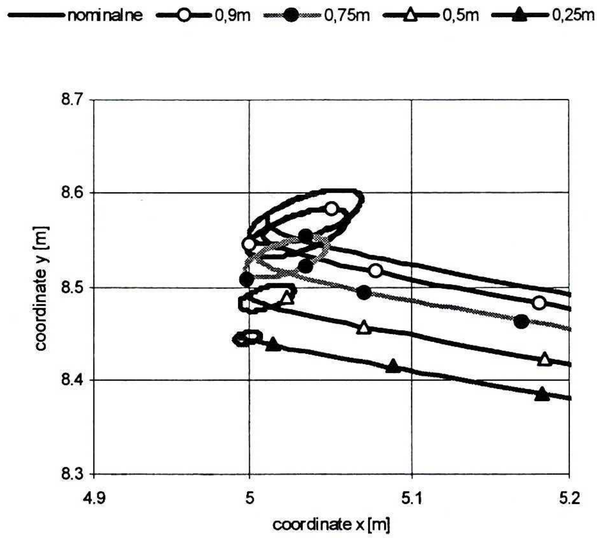


Fig. 31. Trajectories of load for decreased mass – optimal drive function

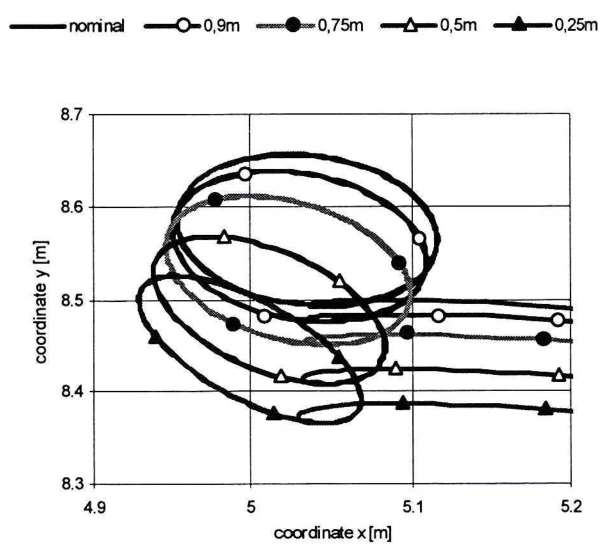


Fig. 32. Trajectories of load for decreased mass – interpolated drive function

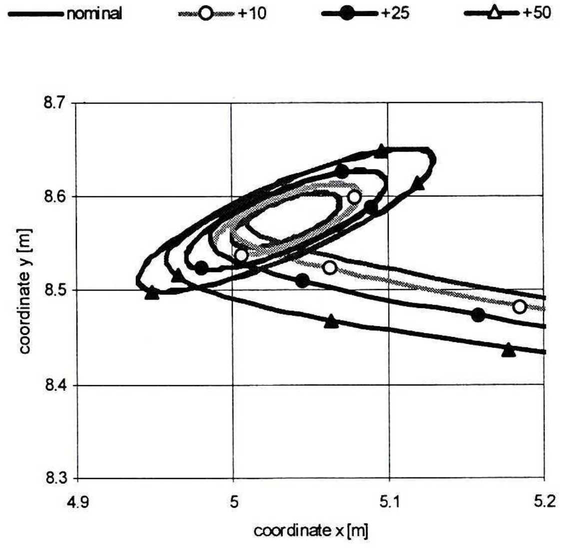


Fig. 33. Trajectories of load for increased length of the rope – optimal drive function

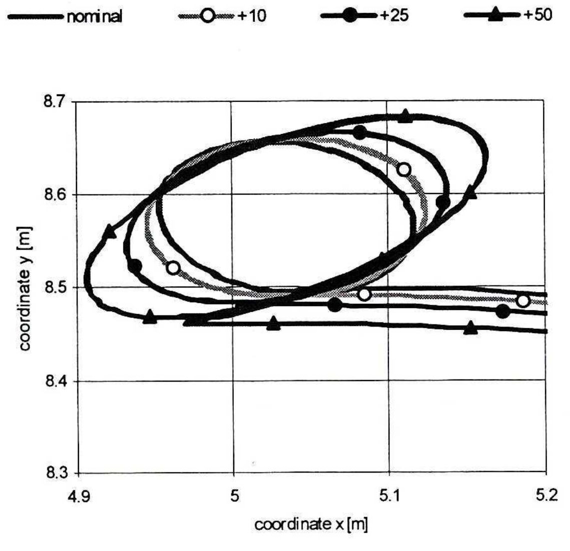


Fig. 34. Trajectories of load for increased length of the rope – interpolated drive function

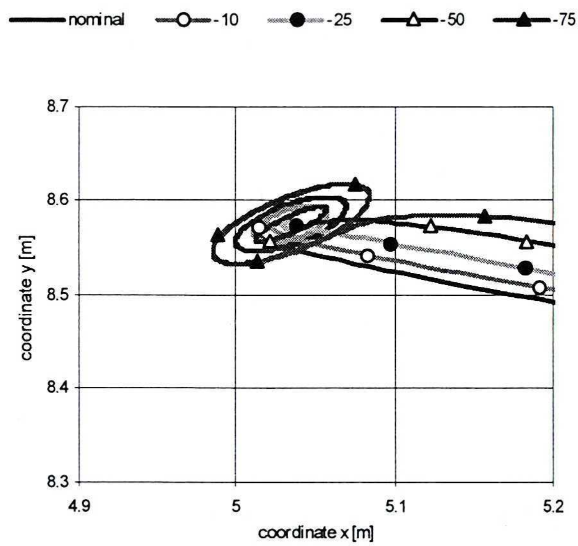


Fig. 35. Trajectories of load for decreased length of the rope – optimal drive function

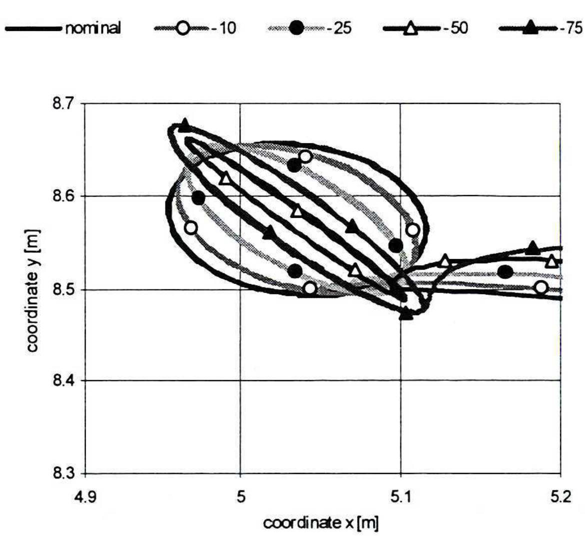


Fig. 36. Trajectories of load for decreased length of the rope – interpolated drive function

After analysing the results for optimal functions presented in sections 6.1 and 6.2, the following conclusions can be formulated:

- the sensitivity of load positioning to changes of mass in the range ±20 % is relatively low,
- the decrease of mass of the load causes reduction of load oscillations at the end of the motion – the greater the reduction, the greater the decrease of mass is,
- the increase of length of the rope by 10 cm causes slight increase of load oscillations. However, when the rope is lengthened by 50 cm then the amplitude of load oscillations at the end of the is about 3 times greater,
- the decrease of length of the rope by 10, 25 and 50 cm causes decrease of final load oscillations. The lowest amplitude of oscillations was obtained for length reduction by 25 cm (for all three angles of slewing),
- when length of the rope is reduced by 75 cm then load oscillations are greater than for the nominal length.

Unfortunately, when input of slewing is performed by means of the interpolated drive function, the results obtained are worse. In this case, the amplitude of load oscillation at the end of the motion for nominal parameters is nearly 3 times greater in comparison to the optimal drive function. The deterioration in load positioning quality is confirmed by an increase in the $P_E$ coefficient value. During slewing by 75° the coefficient is equal to 4.59 cm for the optimal drive function and to 11.67 cm for the interpolated one. Some differences between both inputs can be also seen when sensitivity of positioning is investigated. Above all, decrease of the amplitude of oscillations for decreased mass of the load and, within a certain range, decreased length of the rope is much smaller for the interpolated function than for the optimal one.

## 6.3. Sensitivity investigation for the intermediate angle and the re-determined drive function

As a result of considerations formulated in the previous section the slewing function for 75° was calculated once again. Linear interpolation was used again. However, the basic functions determined previously for 90° and 60° were replaced by functions determined for 80° and 70°. Next, the simulations investigating sensitivity of load positioning to considered parameters were repeated. The same changes of nominal mass of the load and length of the rope were analysed. The following figures (Figs. 37, 38, 39 and 40) show results of calculations. $P_E$ coefficient values obtained are presented in Table 3. Additionally, values of the PE coefficient obtained for the optimal drive function are also quoted in the table in order to facilitate comparison.

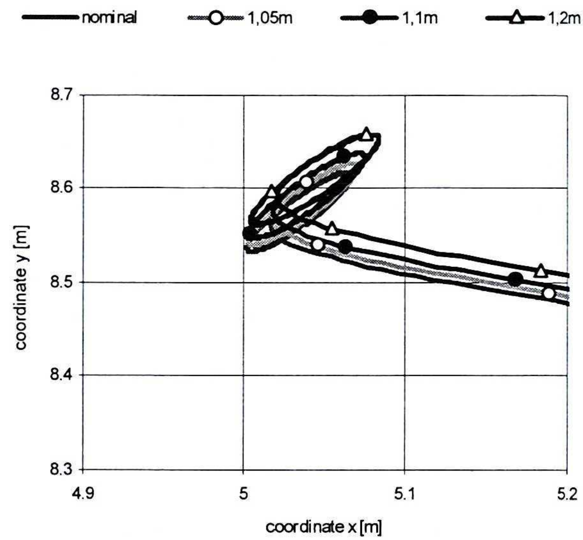


Fig. 37. Trajectories of load for increased mass – second new interpolated drive function

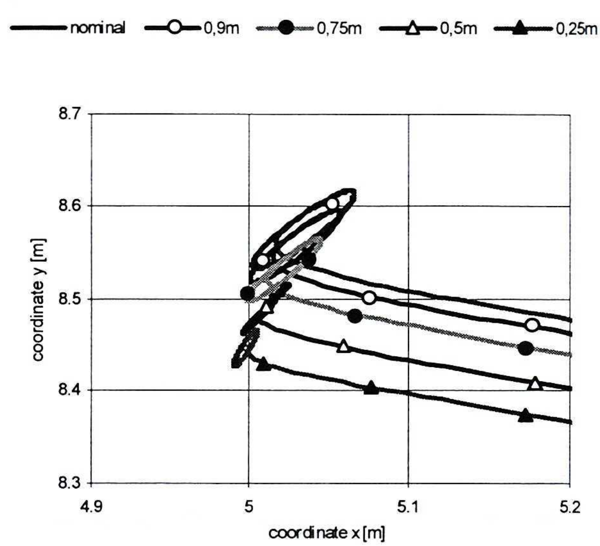


Fig. 38. Trajectories of load for decreased mass – second new interpolated drive function

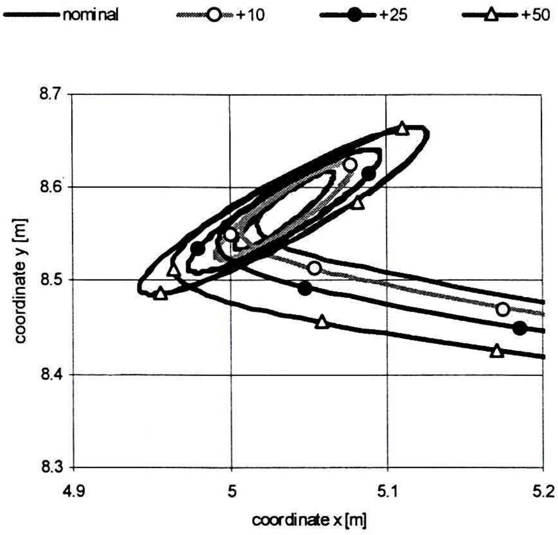


Fig. 39. Trajectories of load for increased length of the rope – new interpolated drive function

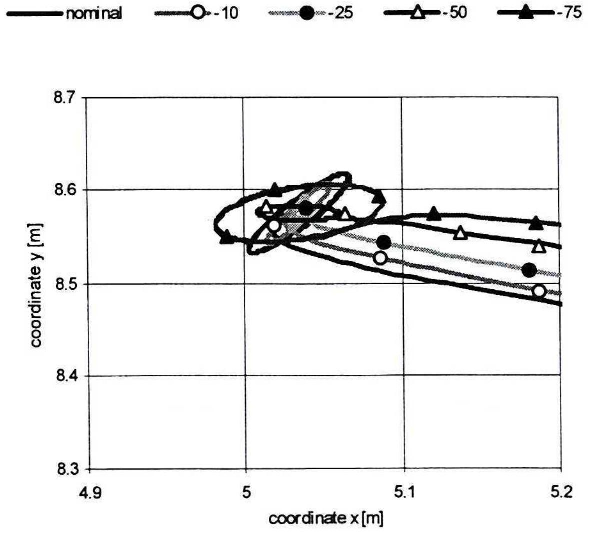


Fig. 40. Trajectories of load for decreased length of the rope – new interpolated drive function

Table 3.
Comparison of $P_E$ coefficient values for the intermediate angle of slewing – 75° and the new interpolated function

| Function | Value of $P_E$ coefficient [cm] | | | | | | | | | | | | | | |
|---|---|---|---|---|---|---|---|---|---|---|---|---|---|---|---|
| | nom. | 1.05m | 1.1m | 1.2m | 0.9m | 0.75m | 0.5m | 0.25m | +10 | +25 | +50 | −10 | −25 | −50 | −75 |
| optm. | 4.59 | 4.77 | 5.05 | 5.51 | 4.08 | 3.39 | 2.23 | 1.12 | 6.09 | 8.37 | 12.2 | 3.10 | 0.95 | 2.98 | 6.57 |
| inter. | 5.35 | 5.53 | 5.80 | 6.25 | 4.89 | 4.18 | 3.11 | 2.19 | 6.83 | 9.10 | 13.0 | 3.90 | 1.96 | 2.76 | 6.20 |

## 7. Final remarks

Results presented in section 3 show the efficiency of the method of determining slewing drive functions based on an optimisation algorithm. For both I and II motions, the load was nearly motionless at the end of slewing. It is proved by Figs. 7 and 8 showing projections of load trajectories, Figs. 9 and 10 showing courses of kinetic energy of the load as well as by the value of the $P_E$ coefficient that is equal to 0.14 cm. The amplitude of load oscillations at the end of the motion was reduced from about 1 m for case I and from 1.7 m for case II to 0.0 m.

Flexibilities of the supported structure of the crane, taken into account in section 4, had slight consequences on the quality of load positioning at the end of the motion. In both cases of slewing, the amplitude of final oscillations for the optimal drive function did not exceed a few centimetres.

In section 5, the slewing function for the intermediate angle was determined using simple linear interpolation. This function is slightly different from the optimal function (Figs. 16 and 17). Load positioning at the end of the motion (Figs. 18 – 20) is also satisfactory.

Detailed conclusions related to the investigation of sensitivity of load positioning at the end of the motion and the input in the form of the optimal drive function are formulated in section 6.2.

In order to investigate sensitivity of positioning when the interpolated function is used as input, slewing by 75° has been assumed. The optimal functions for 60° and 90° were applied to determine this function. During simulations, it was proved that in this case of input, the behaviour for load was less propitious than for the optimal drive function. That is why the drive function was determined once again. The optimal functions for slewing by 70° and 80° were taken as basic functions. This new drive function caused significant improvement in quality of load positioning. The value of the $P_E$ coefficient for nominal mass of the load and length of the rope decreased from 11.67 cm (for basic slewing by 60° and 90°) to 5.35 cm (for basic slewing by 70° and 80°), while the $P_F$ coefficient value for the optimal drive function is equal to 4.59 cm. Sensitivity of load positioning for the new interpolated drive function is similar to sensitivity for the optimal function.

In this paper, a coefficient of load positioning quality $P_E$ is proposed. It is an attempt to quantitative evaluation positioning quality which allows for an easy comparison of the efficiency of different drive functions. It may be especially useful in constructing the „map of basic slewing functions". By determining the boundary admissible value of the coefficient, one can simply calculate ranges of change of mass of the load or change of length of the rope for which satisfactory positioning quality can be obtained using only one drive function.

The most important conclusions about the „map of basic slewing functions" are:

1. By knowing drive slewing functions for selected angles one can, using linear interpolation, determine the drive functions for intermediate angles that ensure satisfactory quality of positioning.
2. By changing the interval between basic points of the map (by determining basic functions for a smaller increment of slewing angles), quality of load positioning at the end of the motion can be considerably improved. Sensitivity of optimal and interpolated functions is then also similar.
3. The drive function may be determined only for maximal mass of the load admissible in a given crane radius. Quality of load positioning for smaller masses is better.
4. One drive function can be used for nominal and also for slightly shorter lengths of the rope.
5. The proposed coefficient $P_E$ reflects well the quality of load positioning and it can be useful constructing the „map of basic functions".

The method presented is helpful especially in controlling cranes that execute certain recurrent operations, for instance those cranes working in reloading railway terminals.

Manuscript received by Editorial Board, January 25.03, 2003
final version, 15.09, 2003.

REFERENCES

[1] Neitzel R. L., Seixas N. S., Ren K. K.: A Review of Crane Safety in the Construction Industry, Applied Occupational and Environmental Hygiene, 2001, vol. 16, no. 12, pp.1106÷1117.

[2] Balachandran B., Li Y.-Y., Fang C.-C.: A Mechanical Filter concept for control of Non-Linear Crane-Load Oscillations, Journal of Sound and Vibration, 1999, 228 (3), pp.651÷682.

[3] Abdel-Rahman E. M., Nayfeh A. H.: Pendulation Reduction in Boom Cranes Using Cable Length Manipulation, Nonlinear Dynamics, 2002, 27 (3), pp. 255÷269.

[4] Sakawa Y., Shindo Y., Hashimoto Y.: Optimal control of a rotary crane', Journal of Optimzation Theory and Applications, 1981, 35, pp. 535÷557.

[5] Kłosiński J.: Slewing Motion Control in Mobile Crane Ensuring Stable Positioning of Carried Load, The Archive of Mechanical Engineering XLVII, Polish Academy of Science, 2000, pp. 119÷138.
[6] Parker G. G., Petterson B., Dohrmann C., Robinett R.D.: Command shaping for residual vibration free crane maneuvers', Proc. American Control Conference, Seattle, Washington, June 1995, pp. 934÷938.
[7] Maczyński A.: Dynamics of a mobile crane in the aspect of steering its drives, Ph.D Thesis, Technical University of Łódź, Branch of Bielsko-Biała, 2000, (in Polish).
[8] Maczyński A., Kościelny R.: A Dynamic Model to Optimisation Working Motions of a Mobile Crane, Proc. Tenth World Congress on the Theory of Machines and Mechanisms, Oulu, Finland, June 20–24, 1999, Vol. 4, pp. 1561÷1566.
[9] Maczyński A., Szczotka M.: Comparison of models for dynamic analysis of a mobile telescopic crane, Journal of Theoretical and Applied Mechanics, 2002, No. 4, Vol 40, pp.1051÷1074.

## Dobór funkcji napędowych obrotu żurawia samojezdnego minimalizujących wahania ładunku

Streszczenie

W pracy przedstawiono metodę doboru funkcji napędowych obrotu nadwozia żurawia samojezdnego. Celem doboru było ograniczenie końcowych wahań ładunku. Przy zastosowaniu prostego modelu żurawia wyznaczono, na drodze optymalizacji, funkcje napędowe dla wybranych kątów i czasów obrotu nadwozia. Funkcje napędowe dla kątów pośrednich określono na drodze interpolacji. Zamieszczono wyniki symulacji numerycznych przeprowadzonych dla modelu żurawia uwzględniającego podatność układu nośnego i tłumienie w wybranych podukładach. Porównano wyniki uzyskane dla funkcji napędowych określonych przy wykorzystaniu algorytmów optymalizacji i interpolacji. Przedstawiono także próbę określenia wrażliwości pozycjonowania ładunku na wybrane parametry eksploatacyjne. Zaproponowano wprowadzenie pojęcia wskaźnika jakości pozycjonowania.